Hittite Journal of Science and Engineering, 2016, 3 (1) 41-49
ISSN NUMBER: 2149-2123
DOI: 10.17350/HJSE19030000031

The Structural and Thermal Characterization of New Cu-Arginate Complex; Experimental and Simulated Hydrogen Adsorbstion Properties

Zarife Sibel Şahin[1], Zeynel Öztürk[2], Ömer Yurdakul[3], Dursun Ali Köse[3]
[1] Sinop University, Department of Energy Systems Engineering, Sinop, TURKEY
[2] Hitit University, Department of Chemical Engineering, Corum, TURKEY
[3] Hitit University, Department of Chemistry, Corum, TURKEY

ABSTRACT

The copper-arginate complex was synthesized and characterized by using FTIR, TG/DTA-DrTG, UV-Vis spectroscopy and elemental analysis methods. In addition, experimental and theoretical hydrogen storage capabilities were investigated. The unit cell of complex structure included that one mole CuII as centered cation and one mole of free NaI cation and one mole of $NaSO_4^-$ as coordinated to arginine ligand and two moles of arginate ligands and one mole of aqua ligand as coordinated to $NaSO_4^-$. The CuII cation had square-pyramidal coordination sphere and the Na1 metal cation had trigonal coordination scheme. The other sodium metal cation (Na2) was implemented in the released position as counter ion of $NaSO_4^-$. It was found that the arginine complex, synthesized in this work have 0.533 m^2/g BET surface area and 6.92E-3 wt. % hydrogen storage capacity at 77 K and 1 bar while simulated value was 3.27E-3 wt. % for the same conditions. .

Article History:
Received: 2016/05/03
Accepted: 2016/06/14
Online: 2016/06/30

***Correspondence to**: Dursun Ali Köse, Hitit University, Faculty of Science and Arts, Department of Chemistry, Corum, TURKEY*
Tel: +90 (364) 270 0000/1643
Fax: +90 (312) 270 0005
E-Mail: dalikose@hitit.edu.tr

Key Words:
Helix Structure; Arginate Complex; Transition Metal Complex; Thermal Decomposition; Electronic Spectra; Cu(II) Complex; X-Ray Diffraction Analysis.

INTRODUCTION

The amino acid molecules are strong Lewis acid base coordinating to metal cation centers. One of them, arginine (Arg), is a very significant amino acid that has guanidium group in side chain, which has basic character at large pH scale. Therefore, it operates as a biological identification site through directed hydrogen bonds [1,2].

The coordination compounds of amino acids or peptides with metal cations are also critical to be model systems for comprehension of biochemical processes in living organisms and some industrial process [3]. The coordination bonding between amino acids and metal cations is well known. This bonding is carried out via a chelate binding mode involving both carboxylate and amine groups, so it is very strong type. [4]. The metal cations support intermolecular coactions by coordinating the interacting molecules in suitable positions [5,6]. Recently, interest to coordination compounds of amino acids with metal cations have been increased because they have confirmed to be useful for some biological applications and material applications for gas absorption [7-9]. Also, the complex compounds of metal cations with bioactive ligands are more influential than pure bioactive compounds most of the time [10,11]. It was explained enough that heterocyclic compounds took an important part in many biological systems [12-15]. Moreover, the anti-bacterial and anti-microbial effect of some drugs could be increased via chelation to center of a metal cation. Herewith, to obtain powerful anti-microbial species, it is very significant to identify about structure and bonding properties of coordination compounds. In many coordination structures of metal ions, carboxylic group bonds with monoanionic and monodentate or bidentate, electron donor amino group coordinates to metal as neutral and monodentate [16-18].

A kind of coordination complex which contain metal and organic building blocks named Metal-Organic Frameworks (MOFs), expressed by Yaghi et al. [19]. The most common application of MOFs is the gas adsorption, especially hydrogen [20]. 1, 2, or 3 dimensional coordination compounds, named MOFs, have advantages on hydrogen storage ability by adjustable pores and electrostatic potential distribution [21, 22]. Many MOFs which were reported previously, were mono ligand and less were mixed ligand complexes. However?, hydrogen storage application of modified mono or mixed ligand complexes have been investigating densely in recent years. Modification of MOFs could bein two ways, which are chemical modification and physical dispersion. Both methods may cause increment on hydrogen storage, that is why the partial charges and porosities of the host material changes by dopants [23]. Chemical modification of the MOFs was also reported as placement of inorganic groups inside the host complex. Chemically modified structures could have different crystal structures and chemical composition in comparison to the unmodified ones.

The possibility of using MOFs as hydrogen storage media have been investigated both experimentally and theoretically [24]. Both methods have advantages. For instance, the weaknesses of the theoretical methods could be solved by the experiments and also theoretical models could be validated by using experimental results. On the other hand, some details which are very hard to measure or analysis experimentally, could be collected theoretically by using simulation calculations. Many of theoretical simulation calculation for hydrogen storage capacity determination of adsorbents realized by using Monte Carlo [25] method. It is reported that the Grand Cannonical Monte Carlo (GCMC) simulation calculations, which is an algorithm collection, had good correlation with the experimental results [26].

Synthesis and characterization of novel arginato complex of copper(II) metal cation studied in this work. In addition, some structural properties of the arginato complex such as molecular orbitals (HOMO; Highest Occupied Molecular Orbitals and LUMO; Lowest Unoccupied Molecular Orbitals) and density of states (DOS), and hydrogen adsorption simulation calculations realized. Molecular structure of arginine ligand was shown in Fig.1.

A similar cupper complex of arginine reported previously [27]. The differences between the present work and previously reported one were the crystal structure. In the present arginine compound, free atomic natrium existed in addition to the coordinated one in the unit cell. Also the present crystal had one dimensional coordination chain while previous had molecular crystal with seconder interactions.

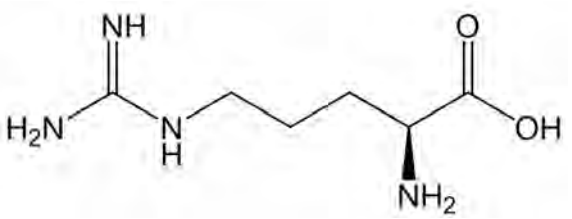

Figure 1. Arginine

EXPERIMENTAL

Materials and measurements

The initial reactants used for synthesis were of reagent grade and CuSO4.5H2O, NaHCO3 and L-arginine (Sigma-Aldrich) were used as received.

Synthesis

Firstly, sodium-arginate salt was obtained according to below reaction formula.

$$2\text{arginine} + 2NaHCO_3 \longrightarrow 2\text{Na(arginate)} + 2CO_2 + 2H_2O$$

For the complex of copper-arginato, copper sulphate salt solution was added to salt-solution of Na-arginate and stirred for a day. The dark-blue precipitates were obtained after one month and they were filtered off and dried in air atmosphere. Chemical components of complex were summarized below in Table 1.

CuII complex contains two molecules of arginato moiety that are directly coordinated to metal ion and one mole NaSO4- that is coordinated to arginato ligand via oxygen atom of C=O group and one mole aqua ligand that is coordinated to Na(I) cation and one mole salt type free Na(I) cation. The square-planar coordination of Cu(II) metal ion was completed by two acidic carboxylic oxygen atoms and two amine nitrogen atoms from arginine. The magnetic data also support square-planar structure (Table 1).

Table 1. Analytical data of Cu(II)-complex.

Complex	*MW g/mol*	*Yield*	*Contents found(calcd.) %*				*Color*	*d.p. °C*	m_{eff} *BM*
			C	*H*	*N*	*S*			
$Na[Cu(Arg)_2NaSO_4(H_2O)]$ $C_{12}H_{28}CuN_8Na_2O_9S$	570	92	25.67 (25.28)	4.73 (4.96)	19.59 (19.66)	5.88 (5.62)	Dark-blue	165	1.57

Crystallography

Suitable crystal of copper complex was selected for data collection, which was performed on a STOE IPDS II diffractometer equipped with a graphite-monochromatic Mo-Kα radiation (λ = 0.71073Å) at 296 K. The structure was solved by direct-methods using SHELXS-97 [32] and refined by full-matrix least-squares methods on F2 using SHELXL-97 from within the WINGX [33] suite of software. All non-hydrogen atoms were refined with anisotropic parameters.

Water H atoms were located in a difference map and refined subject to a DFIX restraint of O-H = 0.83(2)Å. Other H atoms were located from different maps and then treated as riding atoms with C-H distances of 0.97-0.98Å and N-H distances of 0.75-0.90Å. The following procedures were implemented in our analysis: program used for molecular graphics were as follow: MERCURY programs [34]; supramolecular analyses: PLATON [35]. Atomic coordinates have been deposited to the Cambridge Structural Database (http://www.ccdc.cam.ac.uk): CCDC 935805.

Hydrogen and nitrogen adsorption calculations

Hydrogen storage capacity of the arginine complex measured by using adsorption instrument (Quantachrome, Autosorb-IQ, Bayton Beach, FL) in different fugacity steps up to 1 relative pressure, experimentally. Also, the surface area and porosity calculated by using experimentally measured nitrogen adsorption data. Pore size distribution and surface area of the arginine complex calculated according to BJH method and BET theory, respectively. Then, the simulated hydrogen and nitrogen adsorption isotherms collected by using Monte Carlo methods in sorption module of Materials Studio software collection. Monte Carlo calculations realized in different 10 fugacity steps by using Metropolis method within 10 000 equilibration and production steps at 77 K. In addition, the force field, which was modified for the low temperature intermolecular interaction because of the quantum effects, used in the adsorption calculations. The details of the force field modification and the parameters explained deeply in our previous work [28,29]. The simulated model validated with the experimental surface area calculations by using Amorpous Cell module. In the amorpous cell calculations, 3*2*1 super cells dispersed in a new cubic unit to construct semi-crystalline amorpous repeated unit. The structure also been energy minimized while constructing the semi-crystalline amorpous cell according to Monte Carlo method by using force field.

Table 2. Some important FT-IR peaks of Cu(II)-complex.

Groups	*Cu^{II}*
n(OH)$_{H2O}$	*3600-3000*
n(NH$_2$)	*3417, 3149*
n(NH$_2$)$_{bending}$	*1577*
n(C=O)$_{carbonyl}$	*1682*
n(COO-)$_{asym}$	*1634*
n(COO-)$_{sym}$	*1390*
Dn$_{as-s}$	*244*
n(CH$_2$)	*2958*
n(NaSO$_4^-$)	*2877, 1121*
n(C-N)	*745-921*
n(M-N)	*469*
n(M-O)	*596*

RESULTS AND DISCUSSION

Electronic Spectra

The magnetic moment, chemical composition and some properties of new product were given in Table 1. The elemental analysis indicated that complexes had two molecules of arginate ligands and one mole sulphate anion per mole formula unit. The Cu(II) complex structure has square planar geometry. High intensity peak was detected at 311 nm for CuII complex that attributed to the metal -> ligand charge transfer band. The results were agreeable to literature [14-18].

Infrared Spectra

The vibration bands of Cu(II) ion complex was summarized in Table 2. The asymmetric and symmetric stretching vibrations of aqua molecules were observed strong and broad absorption band in the range of 3600-3000 cm^{-1}. At the 3401–3149 cm^{-1}, bands were belonging to N-H stretches of primary amides. The two weak bands at the range of 2877 cm^{-1} was attributed to the CH_2 and at the 2958 and 1121 cm^{-1} peaks were belonging to $NaSO_4^-$ group. The coordination carbonyl group, bonded to metal cations, exhibit strong bands in the region of 1682 cm-1. The asymmetric vibration band of COO- group was appeared at 1634 cm-1, while the symmetric vibration band of COO- group was at 1390 cm^{-1}. The shift (Δ) between of the ν_{asym}. and ν_{sym}. bands of COO- group was at 244 cm^{-1} and it was higher than monoanionic carboxylate group (158 cm^{-1}), so it could be suggested that the COO- group was coordinated to metal(II) cation

Table 3. The thermal analysis data of Cu(II)-complex.

	Na[Cu(arg)$_2$(NaSO$_4$)(H$_2$O)]								*Dark-Blue*
1	*156-161*	*145*	*H$_2$O*	*4.21*	*3.50*			*Na[Cu(arg)$_2$NaSO$_4$]*	
2	*163-810*	*180,207,234, 472*	*2 arg*	*65.34*	*67.19*			*CuO.Na$_2$SO$_4$*	
3	*818-990*	*859*	*SO$_2$*	*7.62*	*8.93*	*78.54*	*77.17*	*CuO.Na$_2$O*	*Black*

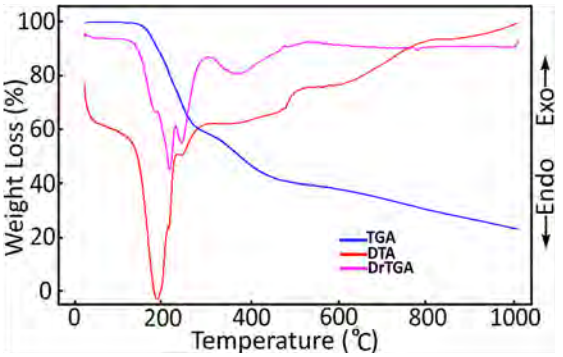

Figure 2. The TG/DTG and DTA curves of Cu(II)-complex.

as monoanionic-bidentate in this structure [30,31]. The vibration of Cu-N interaction was emerging at the 469 cm-1, while ascribed to the Cu-O bands were observed at the 596 cm-1 [18].

Thermal Analysis

The vibration bands of Cu(II) ion complex was summarized in Table 2. The asymmetric and symmetric stretching vibrations of aqua molecules were observed strong and broad absorption band in the range of 3600-3000 cm^{-1}. At the 3401–3149 cm^{-1}, bands were belonging to N-H stretches of primary amides. The two weak bands at the range of 2877 cm^{-1} was attributed to the CH_2 and at the 2958 and 1121 cm^{-1} peaks were belonging to $NaSO_4^-$ group. The coordination carbonyl group, bonded to metal cations, exhibit strong bands in the region of 1682 cm^{-1}. The asymmetric vibration band of COO^- group was appeared at 1634 cm^{-1}, while the symmetric vibration band of COO- group was at 1390 cm-1. The shift (Δ) between of the $\nu_{asym.}$ and $\nu_{sym.}$ bands of COO^- group was at 244 cm^{-1} and it was higher than monoanionic carboxylate group (158 cm^{-1}), so it could be suggested that the COO- group was coordinated to metal(II) cation as monoanionic-bidentate in this structure [30,31]. The vibration of Cu-N interaction was emerging at the 469 cm-1, while ascribed to the Cu-O bands were observed at the 596 cm-1 [18].

Crystallography

A summary of the crystal data, experimental details and refinement results were listed in Table 4. The crystal structure of complex with the atom labeling was shown in Fig. 3. The asymmetric unit of Cu(II) complex consisted of a Cu(II) ion, two Na(I) ions (one of them salt

Table 4. Crystal and refinement data for Cu(II)-complex.

Molecular formula	$C_{12}H_{28}CuN_8Na_2O_9S$
Molecular mass	*570.00*
Crystal system	*Orthorhombic*
Space group	$P2_12_12_1$
Unit cell parameters a, b, c, Å	*7.0483(2), 12.9180(4), 25.4460(7)*
V, Å³	*2316.86(12)*
Z	*4*
ρ_{calc}, *g/cm³*	*1.634*
T, K	*293*
Radiation, λ, Å	MoK_α; *0.71073*
Crystal size, mm	*0.41x0.21x0.03*
Reflections measured	*22093*
$\vartheta_{min, max}$, *deg*	*1.6-27.2*
Independent reflections	*4495* [R_{int} = *0.251*]
Parameters refined	*290*
Final R factor [I > 2σ(I)]	*R1 = 0.104, wR2 = 0.246*
GOOF	*1.02*
Residual electron density (min/max), e/Å³	*-0.75/0.78*

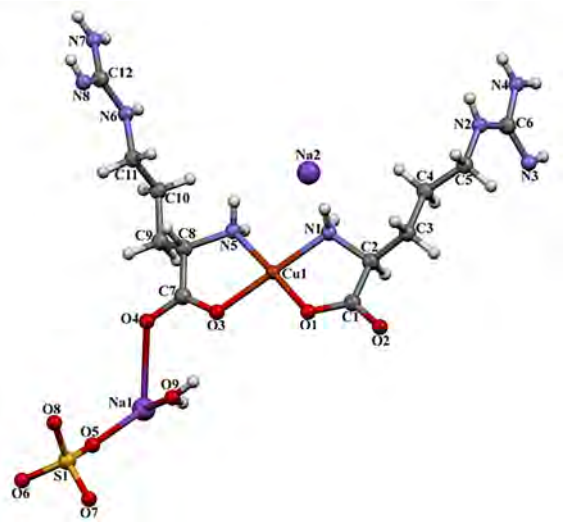

Figure 3. The molecular structure of Cu(II)-complex showing the atom numbering scheme.

type, other one is coordinated), two arginine ligands, one coordinated water molecule and one sulfate anion. The Cu1 exhibits penta-coordination with a distorted square pyramidal geometry. The equatorial coordination came from two oxygen atoms (O1 and O3) and two nitrogen atom (N1 and N5) of two different arginine ligands, while the apical position was occupied by one oxygen atom (O4ii) of different arginine ligand [(ii) x+1/2, -y+3/2, -z+1].

Table 5. Selected bond lengths (Å) and angles (°) for Cu(II)-complex.

Cu(1)-N(1)	*1.964(10)*	*Cu(1)-N(5)*	*1.989(10)*	*Cu(1)-O(1)*	*1.931(8)*
Cu(1)-O(3)	*1.973(9)*	*Cu(1)-O(4)^{ii}*	*2.482(8)*	*Na(2)^{i}-O(2)*	*2.755(17)*
Na(1)-O(4)	*2.62(3)*	*Na(1)-O(5)*	*2.84(3)*	*Na(1)-O(9)*	*2.86(3)*
O(1)-Cu(1)-N(1)	*84.2(4)*	*O(1)-Cu(1)-O(3)*	*93.8(3)*	*N(1)-Cu(1)-O(3)*	*177.1(4)*
O(1)-Cu(1)-N(5)	*175.8(4)*	*N(1)-Cu(1)-N(5)*	*98.0(4)*	*O(3)-Cu(1)-N(5)*	*84.0(4)*

Symmetry codes: (i) x+1/2, +y+1/2, +z+1; (ii) x+1/2, -y+3/2, -z+1.

Table 6. Hydrogen bonds for Cu(II)-complex.

D-H···A	D-H (Å)	H···A (Å)	D···A (Å)	D-H···A (°)	Symmetry operations
N(1)-H(1A)···O(5)	0.90	2.26	3.115 (14)	159	x, y, z
N(2)-H(2)···O(7)	0.86	2.05	2.900 (14)	168	−x+1, y−1/2, −z+3/2
N(3)-H(3)···O(7)	0.75	2.30	3.040 (13)	170	−x+2, y−1/2, −z+3/2
N(4)-H(4C)···O(5)	0.86	2.48	3.268 (16)	153	−x+2, y−1/2, −z+3/2
N(4)-H(4C)···O(7)	0.86	2.55	3.281 (15)	144	−x+2, y−1/2, −z+3/2
N(4)-H(4D)···O(8)	0.86	2.05	2.890 (15)	165	−x+1, y−1/2, −z+3/2
N(5)-H(5C)···O(8)	0.90	2.16	2.901 (14)	139	x, y, z
N(5)-H(5D)···O(9)	0.90	1.99	2.89 (2)	178	x, y, z
N(6)-H(6)···O(6)	0.86	1.95	2.803 (18)	174	−x+1, y+1/2, −z+3/2
N(6)-H(6)···S(1)	0.86	2.81	3.526 (12)	142	−x+1, y+1/2, −z+3/2
N(7)-H(7B)···O(5)	0.86	2.30	3.037 (17)	143	−x+1, y+1/2, −z+3/2
N(8)-H(8A)···O(6)	0.75	2.28	2.98 (2)	156	−x, y+1/2, −z+3/2

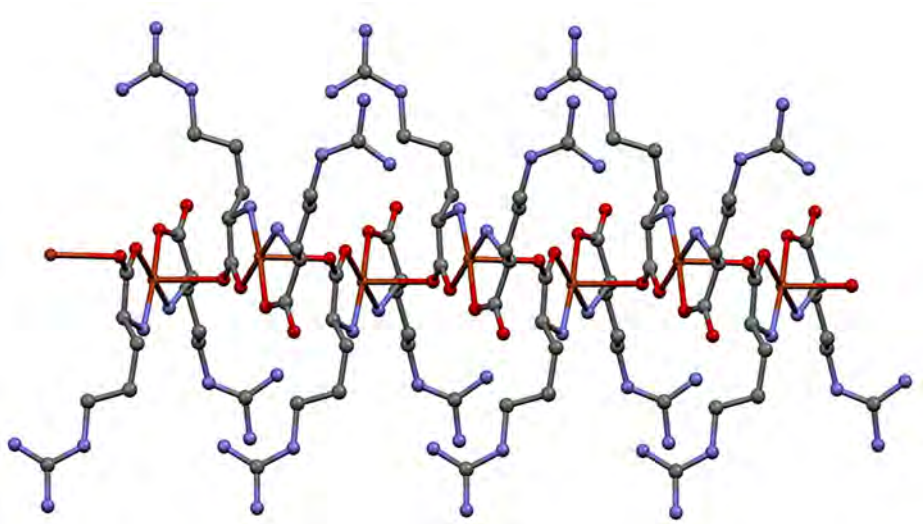

Figure 4. An infinite 1D layer in Cu(II)-complex..

According to the Addison definition, the value of τ for Cu1 is 0.02 [τ = (177.10-175.80) / 60 = 0.02], respectively (τ = 0 for an ideal square-pyramid, τ = 1 for an ideal trigonal-bipyramid) [36].

The Cu(II) ions were bridged by arginine ligands to generate 1D coordination polymer running parallel to the [100] direction (Fig. 4). The Cu1···Cu1ii separation was 5.778 Å. The interpenetration in Cu(II) complex was reinforced by N-H···O hydrogen bonds between the parallel 1D layers (Fig. 5.a). The Cu-N bond lengths of 1.964(10) and 1.989(10) Å were practically similar to those found in $[Cu(L\text{-}Arg)_2](SO_4)\cdot 6H_2O$ (1.964(5) and 1.991(4) Å), $[Cu(L\text{-}arg)_2(H_2O)]_2(P_4O_{12})\cdot 8H_2O$ (1.971(5) and 1.975(5) Å), $[Cu(argininate)_2(H_2O)]CO_3\cdot H_2O$ (1.977(4) and 1.991(4) Å) [37], but somewhat shorter than those found $\{[Cu_2(L\text{-}arg)_2(Bpy)_2(\mu 2\text{-}ClO_4)_2]\cdot 2ClO_4\cdot 4H_2O\}n$ (1.998(6) and 2.001(6) Å) [38] and $[Cu_2(L\text{-}arg)_2(\mu\text{-}HPO_4\text{-}O)(\mu\text{-}HPO_4\text{-}O,O')(l\text{-}OH)]\cdot\cdot(H_3O)+\cdot 6H_2O$ (1.995(4) and 2.011(4) Å). The equatorial Cu-O bond distances (1.931(8) and 1.973(9) Å) were comparable corresponding distances found in $[Cu(L\text{-}arg)_2(H_2O)]_2(P_4O_{12})\cdot 8H_2O$ (1.946(5) and 1.957(5) Å) [39], $[Cu(argininate)_2(H_2O)]CO_3\cdot H_2O$ (1.947(3) and 1.966(3) Å) [40] and trans-$[Cu(l\text{-}Arg)_2(NO_3)]NO_3\cdot 3H_2O$ (1.936(4) and 1.956(4) Å) [41], while the axial Cu-O bond length (2.482(8) Å) was in agreement with the corresponding value in $\{cis\text{-}[Cu(L\text{-}Arg)_2](NO_3)_2\cdot 3H_2O\}n$ (2.487(2) Å) [42]. Selected bond lengths and angles of structure were given in Table 5.

Atoms N2 and N4 in the molecule at (x, y, z) acts as hydrAtoms N2 and N4 in the molecule at (x, y, z) acted as hydrogen-bond donors, via atoms H2 and H4D, respectively, to atoms O7 and O8 at (-x+1/2, -y+1, z+1/2), so forming

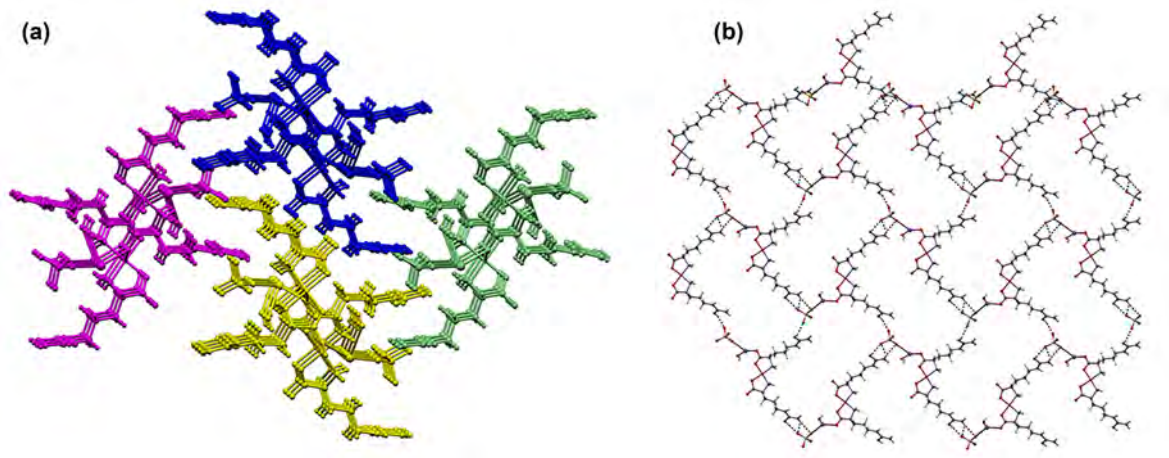

Figure 5. (a) The packing structure of Cu(II)-complex built by four interpenetrated, (b) part of the crystal structure of Cu(II)-complex, showing the N-H···O hydrogen bonds.

C(15) and C(17) [R22(8)] chains running parallel to the [001] direction. Similarly, atoms N3 and N4 in the molecule at (x, y, z) acted as hydrogen-bond donors, via atoms H3 and H4C, respectively, to atoms O7 and O5 at (-x+3/2, -y+1, z+1/2), so forming C(15) and C(17) [R12(4)R21(6)] chains running parallel to the [001] direction. The combination of N-H···O hydrogen bonds produce R44(51) rings running parallel to the [111] direction (Fig. 5.b). The 1D coordination polymer was extended into a three-dimensional frameworks by N-H···O hydrogen bonds (Table 6).

Hydrogen and nitrogen adsorption capacities

BET surface area and pore size distribution of the arginine complex calculated and the plots given in Figure 6. Experimental and simulated nitrogen adsorption isotherms showed Type-III isotherms according to IUPAC classification. The type of isotherms represented micro and meso-porosity existence, in addition adsorbed multilayer formation. Micro and meso-porosity were clearly shown in the pore size distribution plot in Figure 6b. It was also understood that the arginine complex have bigger meso-pores in comparison to micro-pores. Calculated BET surface area was 0.533 m^2/g that could be approved as the structure had small porosity when the value compared to surface areas of the common MOFs.

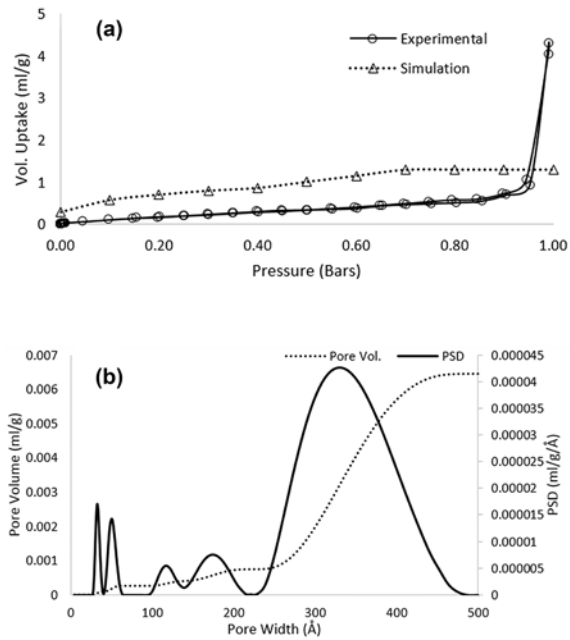

Figure 6. **(a)** Simulated and experimentally collected nitrogen adsorption isotherms and **(b)** pore size distribution of arginine complex.

The simulated and experimental nitrogen adsorption isotherms were similar. While constructing semi crystalline amorphous cell by using relaxed 2x1x1 non-periodic super structure (Figure 7.a), different densities collected but the final structure with 1.3426 g/ml selected as the finest model, which represent the real complex. Crystal density of synthesized complex was 1.5824 g/ml, so the close densities investigated. Semi crystalline amorphous cell used because the crystal structure that was simulated by using cif (crystal information file) did not have any empty spaces. Hence the crystal structure was not able to adsorb both hydrogen and nitrogen. It was shown that the materials used for experimental gas adsorption measurements, had crystal cracks and deformed crystal structures. That is why, representing structure in amorphous cell with crystal building units was wise. Final structure that was used for gas adsorption calculations represented in Figure 7.b. Yellow dots in Figure 7.b represents the surfaces that the hydrogen molecules could be stored. It was also shown that the spaces which possibly uptake hydrogen molecules were small.

Hydrogen molecules in the amorphous cell after adsorption process simulated and given in Figure 8. Green ellipsoids represent the hydrogen molecules.

Hydrogen adsorption isotherms of arginine complex

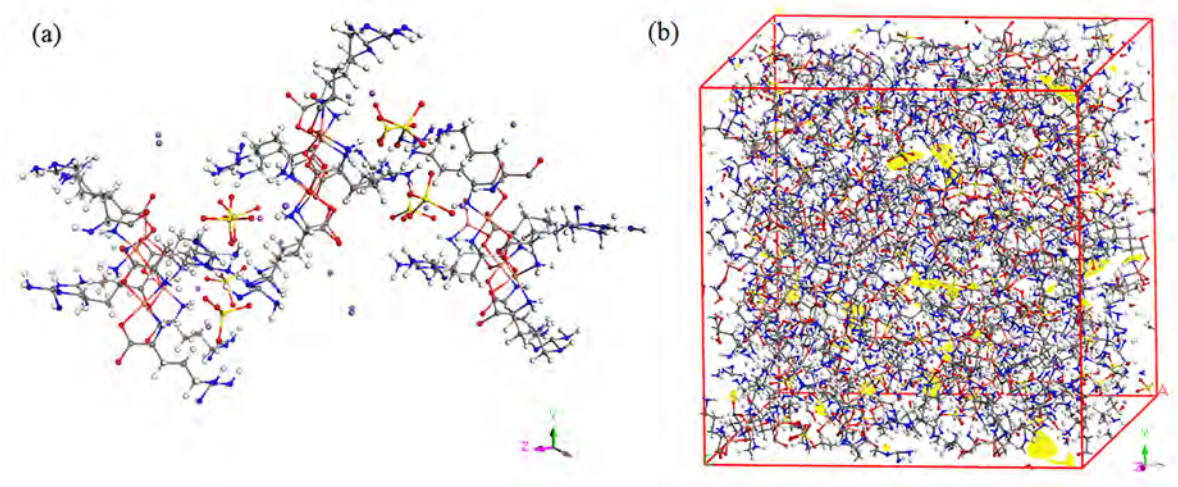

Figure 7. **(a)** 2x1x1 relaxed unit and **(b)** relaxed 10 unit included semi-crystalline amorpous cell.

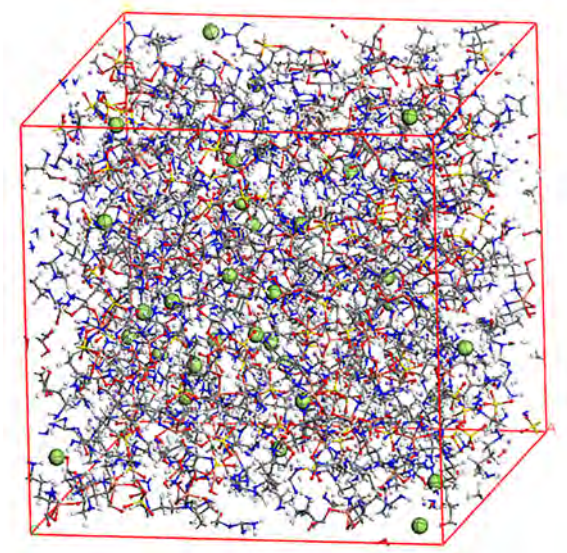

Figure 8. Hydrogen adsorbed arginine structure.

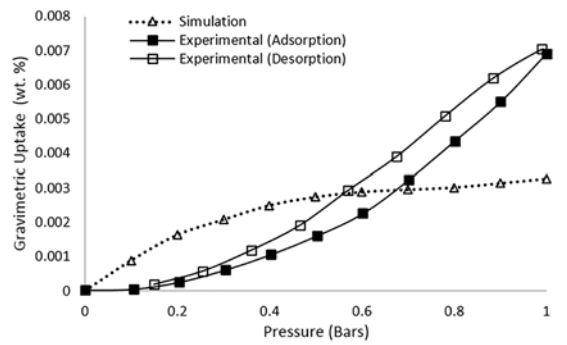

Figure 9. Experimental and simulated hydrogen adsorption isotherms.

both experimental and simulation was given in Figure 9. It was clear that the hydrogen storage adsorption isotherm types differed for simulation and experimental measurements. The main reason of the situation would be the possible residue in the experimental materials. In addition, Monte Carlo calculation could be failed in such small porosity because the force field used for the calculations could not meet the cutoff accuracy for the calculations.

The final hydrogen storage capacity of the arginine complex was 6.92E-3 wt. % at 77 K and 1 bar while simulated value was 3.27E-3 wt. % for the same conditions. In the previous work, different arginine complex was synthesized and also the hydrogen storage capacity was measured. It was found that the previous arginine compound could been adsorbed approximately 0.8 wt. % hydrogen at 77 K and 1 bar pressure [28,29]. The value was 10 times bigger than the present work because the molecular spaces in the present work filled with the free and coordinated natrium and sulfite molecules.

CONCLUSION

The new arginine metal complex "natrium[(natrium(I) sulphate-monoaqua) (bisarginato-κ-O, κ-N) copper(II)]" was synthesized and characterized as structural. The unit cell of complex included two mole arginato and one mole aqua ligands, one mole natrium(I) and copper(II) cations, one mole sulphate anion. One mole natrium cation was settled outside of the unit cell as counter ion. The geometry of complex was square-planar so violence of electronic transitions was weak. The structure of complex was thermally stable until 165°C. The infrared results explained bonding properties of arginine ligands. Both experimental and simulation calculations showed that the hydrogen storage capability of the arginine complex decreased because the empty spaces filled free and coordinated natrium and sulfite molecules. In conclusion, other possible arginine complexes could be investigated to improve hydrogen storage capacity.

ACKNOWLEDGEMENTS

This research was supported by the Science Research Department of Hitit University (Project no: FEF03.12.05).

REFERENCES

1. Cotton FA, Day VW, Hazen EEJr, Larsen S, Wong STK. Structure of bis(methylguanidinium) monohydrogen orthophosphate. Model for the arginine–phosphate interactions at the active site of staphylococcal nuclease and other phosphohydrolytic enzymes J. Am. Chem. Soc. 96 (1974) 4471–4478.
2. Patthy L, Smith EL. Reversible modification of arginine residues. Application to squence studies by restriction of tryptic hyrolysis to lysine residues. J. Biol. Chem. Soc. 250(2) (1975) 557–564.
3. Lippard SJ, Berg JM. Principles of bioinorganic chemistry, (University Science Books), Mill Valley, CA, 1994.
4. Stone DL, Smith DK, Whitwood AC. Copper amino–acid complexes–towards encapsulated metal centres. Polyhedron 23 (2004) 1709–1717.
5. Ohata N, Masuda H, Yamauchi O. Aromatic carboxylate–controlled self–organization of copper(II)-l–arginine complexes. Inorg. Chim. Acta 286(1) (1999) 37–45.
6. Hamilton AD. Supramolecular control of structure and reactivity, Wiley, Chichester, 1996.
7. Stanila A, Marcu A, Rusu D, Rusu M, David L. Spectroscopic studies of some copper(II) complexes with amino acidsJ. Mol. Struc. 834–836 (2007) 364–368.
8. Iqbal MZ, Khurshid S, Iqbal MS. Antibacterial activity of copper–amino acid complexes. J. Pak. Med. Assoc. 40(9) (1990) 221–222.
9. Venelinov T, Arpadjan S, Karadjova I, Beattie. J. Properties of the copper(II)–histidine complex obtained after dialysis of human plasma with histidine. Acta Pharm. 56 (2006) 105–112.
10. Sorensen JRJ, Sigel H. Metal Ions in Biological Systems, Marcel Dekker, New York, Vol. 14, p.77. 1982.
11. Kato M, Muto Y. Factors affecting the magnetic properties of dimeric copper(II) complexes. Coord. Chem. Rev. 92 (1988) 45–83.
12. Nagar R. Synthesis, spectral characterization and DNA bindings of tridentate N_2O donor Schiff base metal(II) complexes. J. Inorg. Biochem. 40 (1990) 349–356.
13. Cavigiolio G, Benedetto L, Boccaleri E, Colangelo D, Viano I, Osella D. Pt(II) complexes with different N–donor aromatic ligands for specific inhibition of telomerase. Inorg. Chim. Acta 305 (2000) 61–68.
14. Öztürkkan EF, Köse DA, Necefoglu H, Uzun I. Synthesis and characterization of bis(N,N–diethylnicotin–amide) p–halogenobenzoate complexes of Co(II). Asian J. Chem. 19(6) (2007) 4880–4888.
15. Köse DA, Gökçe G, Gökçe S, Uzun I. bis(N,N–diethylnicotinamide) p–chlorobenzoate complexes of Ni(II), Zn(II) and Cd(II). J. Therm. Anal. Cal. 95(1) (2009) 247–251.
16. Köse DA, Ay AN, Şahin O, Büyükgüngör O. A mononuclear Zn(II) complex of mixed ligands with both fivefold– and sixfold– coordinations in the same framework J. Iran. Chem. Soc. 9(4) (2012) 591–597.
17. Köse DA, Necefoglu H, Sahin O, Büyükgüngör O. Synthesis, spectral, thermal and structural study of monoaquabis(acetylsalicylato–κO)bis(nicotinamide–κN) copper(II). J. Chem. Crystallogr. 41 (2011) 297–305
18. Köse DA, Zumreoglu–Karan B, Unaleroglu C, Sahin O, Buyukgungor O. Synthesis and characterization of transition metal–vitamin B13 complexes with a Co–vitamin. J. Coord. Chem. 789 (2006) 147–151.
19. Yaghi OM, Li H, Groy TL. Construction of porous solids from hydrogen–bonded metal complexes of 1,3,5–benzenetricarboxylic acid. J. Am. Chem. Soc. 118(38) (1996) 9096–9101.
20. Rosi NL, Eckert J, Eddaoudi M, Vodak DT, Kim J, O'Keeffe M, Yaghi OM. Hydrogen storage in microporous metal–organic frameworks. Science 300(5622) (2003) 1127–1129.
21. Seo JS, Whang D, Lee H, Im Jun S, Oh J, Jeon YJ, Kim K. A homochiral metal–organic porous material for enantioselective separation and catalysis. Nature 404(6781) (2000) 982–986.
22. Sagara T, Klassen J, Ganz E. Computational study of hydrogen binding by metal–organic framework–5. J. Chem. Phys. 121(24) (2004) 12543–12547.
23. Baykasoglu C, Ozturk Z, Kirca M, Celebi AT, Mugan A, To AC. Effects of lithium doping on hydrogen storage properties of heat welded random CNT network structures. Int. J. Hyd. Energy 2016, 41(19), 8246–8255.
24. Ozturk Z, Baykasoglu C, Kirca M. Sandwiched graphene–fullerene composite: A novel 3–D nanostructured material for hydrogen storage. Int. J. Hyd. Energy 41(15) (2016) 6403–6411.
25. Vlachy V, Ichiye T, Haymet ADJ. Symmetric associating electrolytes: GCMC simulations and integral equation theory. J. Am. Chem. Soc. 113(4) (1991) 1077–1082.
26. Pham T, Forrest KA, Hogan A, Tudor B, McLaughlin K, Belof JL, Eckert J, Space B. Understanding hydrogen sorption in In–soc–MOF: A charged metal–organic framework with open–metal sites, narrow channels, and counterions. Cryst. Growth & Design 15(3) (2015) 1460–1471.
27. Köse DA, Toprak E, Kaşarcı A, Avcı E, Avcı GA, Şahin O, Büyükgüngör O. Synthesis, spectral, thermal studies of Co(II), Ni(II), Cu(II) and Zn(II)–arginato complexes. Crystal structure of monoaquabis(arginato–κO, κN)copper(II). $[Cu(arg)_2(H_2O)].NaNO_3$, J. Chin. Chem. Soc. 61 (2014) 881–890.
28. Ozturk Z, Kose DA, Asan A, Ozkan G. Porous metal–organic Cu(II) complex of L–Arginine; synthesis, characterization, hydrogen storage properties and molecular simulation calculations. Hittite J. Sci. & Eng. 1(1) (2014) 1–5.
29. Ozturk Z, Ozkan G, Kose DA, Asan A. Experimental and simulation study on structural characterization and hydrogen storage of metal organic structured compounds. Int. J. Hyd. Energy 41(19) (2016) 8256–8263.

30. Köse DA, Necefoglu H, Icbudak H. Synthesis and characterization of N,N−diethylnicotinamide−acetylsalicylato complexes of Co(II), Ni(II), Cu(II), and Zn(II). J. Coord. Chem. 61(21) (2008) 3508−3515.
31. Köse DA, Necefoglu H. Synthesis and characterization of bis(nicotinamide) m−hydroxybenzoate complexes of Co(II), Ni(II), Cu(II) and Zn(II). J. Therm. Anal. Cal. 93(2) (2008) 509−514.
32. Farrugia LJJ. WinGX suite for small−molecule single−crystal crystallography. Apply. Cryst. 32 (1999) 837−838.
33. Sheldrick GM. A short history of SHELX. Acta Cryst. A64 (2008) 112−122.
34. Mercury, version 3.0; CCDC, available online via ccdc.cam.ac.uk/products/mercury.
35. Spek AL. PLATON−a multipurpose crystallographic tool. Utrecht University, Utrecht (2005).
36. Addison AW, Rao TN, Reedijk J, Rijn JV, Verschoor GC. Synthesis, structure, and spectroscopic properties of copper(II) compounds containing nitrogen−sulphur donor ligands; the crystal and molecular structure of aqua[1,7−bis(N−methylbenzimidazol−2′−yl)−2,6−dithiaheptane] copper(II) perchlorate. J. Chem. Soc. Dalton Trans. (1984) 1349−1356.
37. Ohata N, Masuda H, Yamauchi O. Dianion−controlled supramolecular assembly of copper(II)−arginine complex ion. Inorg. Chim. Acta 749 (2000) 300−302.
38. Hemissi H, Nasri M, Abid S, Al−Deyab SS, Dhahri E, Hlil EK, Rzaigui M. Crystal structure, spectroscopic, magnetic and electronic structure studies of a novel Cu(II) amino acid complex $[Cu(l-arg)_2(H_2O)]_2(P_4O_{12}).8H_2O$. J. Solid State Chem. 196 (2012) 489−497.
39. Viera I, Torre MH, Piro OE, Castellano EE, Baran EJ. Structural and spectroscopic characterization of aqua−diargininate−copper(II)−carbonate monohydrate. J. Inorg. Biochem. 99(5) (2005) 1250−1254.
40. Zhou X, Yang C, Le X, Chen S, Liu J, Huang Z. Synthesis and crystal structures of one−dimensional ClO bridged coordination polymers: $\{[Cu(Bpy)_2(\mu^2-ClO_4)].ClO_4\}$ n and $\{[Cu_2(L-arg)_2(Bpy)_2(\mu^2-ClO_4)_2].2ClO_4{\cdot}4H_2O\}_n$. J. Coord. Chem. 57(5) (2004) 401−409.
41. Santana RC, Carvalho JF, Vencato I, Napolitano HB, Bortoluzzi AJ, Barberis GE, Rapp RE, Passeggi MCG, Calvo R. Synthesis, crystal structure and magnetic properties of a new dinuclear copper(II) amino acid complex $[Cu_2(l-arg)_2(\mu-HPO_4-O)(\mu-HPO_4-O,O')(\mu-OH)]^-.(H_3O)^+.(H_2O)_6$. Polyhedron 26(17) (2007) 5001−5008.
42. Hu R, Yu Q, Liang F, Ma L, Chen X, Zhang M, Liang H, Yu K. Syntheses and crystal structures of cis− and trans−copper(II) complexes of L−arginine. J. Coord. Chem. 61 (2008) 1265−1271.